STATUS OF EXPERIMENTS AND RECENT RESULTS FROM CMD-2 DETECTOR AT VEPP-2M

A.I. Milstein
(CMD-2 collaboration)
Budker Institute of Nuclear Physics, Novosibirsk, 630090, Russia

Abstract

The Cryogenic Magnetic Detector (CMD-2) is shortly described. Preliminary results for the cross sections of $e^+ \ e^-$ annihilation into hadrons and leptons are presented in the c.m. energy range from 0.37 to 1.39 GeV. The total integrated luminosity of about 26 pb^{-1} has been collected. The new results for the ρ and ω meson parameters are reported. The major decay modes of the ϕ meson as well as its rare decays have been observed.

1 Introduction

The investigation of the reaction of e^+e^- annihilation into hadrons at low energies accounts about thirty years history of the experimental studies. Nevertheless, the understanding of the field is still rather far from the completeness. More precise measurements of the ρ-, ω- and ϕ-meson parameters are needed as well as properties of the continuum which provide unique information about interaction of light quarks and spectroscopy of their bound states. The knowledge of the total cross section of e^+e^- annihilation into hadrons at low energies and the magnitude of the exclusive cross sections is also necessary for precise calculations of various quantities. One of them is the strong interaction contribution into anomalous magnetic momentum of muon $(g-2)_\mu$. Tab. 1 shows contributions of various channels into $(g-2)_\mu$ (details of calculations can be found in[1] and[2]). One can see, that the main contribution (about 87%) comes from the energy region below 1.4 GeV and the dominant contribution (71%) in this region is from the channel $e^+e^- \to \pi^+\pi^-$.

The energy behavior of cross section of the process $e^+e^- \to hadrons$ at low energies is rather complicated. It is characteristic of various resonances (ρ, ω, ϕ and their recurrences) and onsets of the separate hadronic channels. Thus, to

Table 1: *Hadronic contributions to the muon* $(g-2)_\mu$

Mode	< 1.4 GeV		> 1.4 GeV	
	$\times 10^{-10}$	%	$\times 10^{-10}$	%
$\pi^+\pi^-$	502.2	71	0.78	0.1
$\pi^+\pi^-\pi^0$	50.96	7.2	0.67	0.1
K^+K^-	20.62	2.9	2.21	0.7
$K_S K_L$	0.76	0.1	14.22	2.0
$\pi^+\pi^-\pi^0\pi^0$	10.78	1.5	8.54	1.2
$\pi^+\pi^-\pi^+\pi^-$	5.16	0.7	10.22	1.5
$\pi^+\pi^-\pi^+\pi^-\pi^0\pi^0$			5.09	0.7
$\pi^+\pi^-\pi^+\pi^-\pi^0$	0.31		2.53	0.4
$K_S K^\pm \pi^\mp$			0.951	0.1
$K^+K^-\pi^+\pi^-$			0.815	0.1
$K^* K^\pm \pi^\mp$			0.692	0.1

determine the value of the total cross section of e^+e^- annihilation into hadrons, one need to measure individual channels one by one and study decay modes of ω and ϕ mesons.

These physical tasks became the goal of the general-purpose detector CMD-2[3] which has been running at the VEPP-2M e^+e^- collider[4] in Novosibirsk since 1992 studying the c.m. energy range from threshold of hadron production to 1.4 GeV.

The CMD-2 detector is described in detail elsewhere[3]. It is a general purpose detector consisting of a drift chamber (DC)[5] with about 250 μ resolution in the plane transverse to the beam axis and multiwire proportional chamber (ZC)[6] with an accurate measurement ($\sim$0.5 mm) of the z-coordinate of particle track along the beam direction. Both chambers are inside a thin (0.38 X_0) superconducting solenoid with a field of 1 T.

The barrel calorimeter placed outside of the solenoid and consists of 892 CsI crystals[7] of $6 \times 6 \times 15$ cm^3 size. The crystals are arranged in eight octants. The light readout is performed by PMTs. The energy resolution is about 8% for photons with the energy more than 100 MeV. Both azimuthal and polar angle resolution is about 0.02 radian.

The endcap calorimeter[8] consists of 680 BGO crystals of $2.5 \times 2.5 \times 15$ cm^3 size. The light readout is performed by vacuum phototriodes placed on the crystals. The energy and angular resolution were found to be $\sigma_E/E = 4.6\%/\sqrt{E(GeV)}$ and $\sigma_{\phi,\theta} = 2 \cdot 10^{-2}/\sqrt{E(GeV)}$ radians respectively. The solid angle covered by both parts of the calorimeter is about 96% of 4π.

The muon range system[9] consists of two double layers of the streamer tubes operating in a self-quenching mode and is aimed to separate pions and muons. The inner and outer parts of this system are arranged in 8 modules each and cover 55% and 48% of the solid angle respectively.

2 Measurement of the pion form factor and ρ, ω meson parameters

A large data sample of about 2 million $e^+e^- \to \pi^+\pi^-$ events was collected by CMD-2 detector in the energy range from 0.360 to 1.370 GeV. Analysis is completed for 10% of the data only. The beam energy was measured by the resonance depolarization technique at almost all energies. The pion form factor presented in fig.1 is based on the data sample at 53 energy points in the energy range from 0.37 to 0.96 MeV. The obtained ρ meson parameters based on Gounaris-Sakurai parametrization were found to be:
$\boldsymbol{M_\rho} = \mathbf{775.28 \pm 0.61 \pm 0.20}$ MeV, $\boldsymbol{\Gamma_\rho} = \mathbf{147.70 \pm 1.29 \pm 0.40}$ MeV,
$\boldsymbol{\Gamma_{\rho \to e^+e^-}} = \mathbf{6.93 \pm 0.11 \pm 0.10}$ keV,
$\boldsymbol{Br(\omega \to \pi^+\pi^-)} = \mathbf{(1.31 \pm 0.23 \pm 0.02)}\%$.
Here and below the first errors are statistical and the second are systematic. More details about the pion form factor can be found in[10].

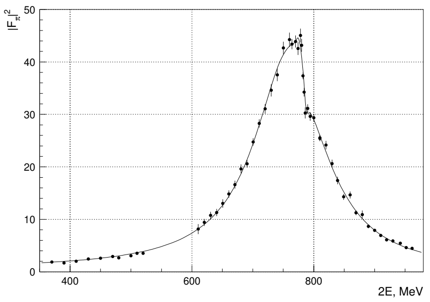

Figure 1: *The pion form factor vs c.m.energy and the fit with Gounaris-Sakurai parametrisation .*

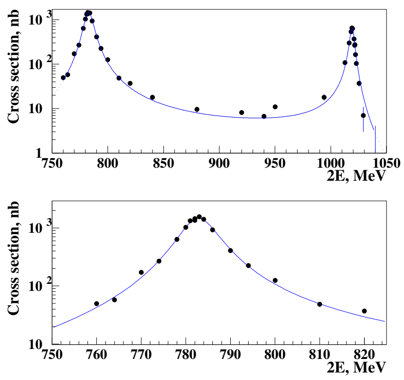

Figure 2: *The upper figure - cross section vs c.m.energy and common fit for the ω, ϕ mesons. The lower figure - cross section in the energy range around ω-meson.*

The energy range around the ω meson has been scanned at 13 energy points with a total integrated luminosity of about 1.5 pb^{-1}, but the detailed analysis

was performed for 10% of the data. The ω meson parameters were measured with high accuracy using the $\omega \to \pi^+\pi^-\pi^0$ decay mode. The following parameters have been obtained from the fit:
$\boldsymbol{M_\omega = 782.71 \pm 0.07 \pm 0.04}$ MeV, $\boldsymbol{\sigma_0 = 1482 \pm 23 \pm 25}$ nb,
$\boldsymbol{\Gamma_\omega = 8.68 \pm 0.23 \pm 0.10}$ MeV, $\boldsymbol{\Gamma_{e^+e^-} = 0.605 \pm 0.014 \pm 0.010}$ keV.
The common excitation curve for the ω and ϕ meson is presented in fig.2.

3 Measurements of ϕ meson parameters

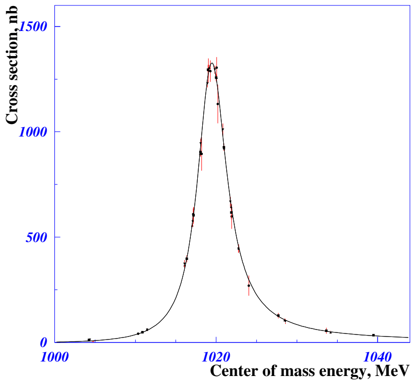

Figure 3: *Experimental cross section and ϕ meson excitation curve in the channel $e^+e^- \to K^0_L K^0_S$*

The ϕ-meson parameters were measured using data on the four major decay modes of $\phi \to K_S K_L$, K^+K^-, 3π, $\eta\gamma$. The first results based on a relatively small integrated luminosity of about 300 nb^{-1} were published in[11]. The new more precise results were obtained for the channel $\phi \to K^0_L K^0_S$ when K^0_S decays into a $\pi^+\pi^-$[12]. The data sample was collected in four scans of the energy range from 984 to 1040 MeV with the integrated luminosity of 2.37 pb^{-1} and contains 2.97×10^5 of selected $K^0_L K^0_S$. Fig.3 shows energy dependence of the cross section of the reaction $e^+e^- \to K^0_L K^0_S$ and the excitation curve of the ϕ meson. The following parameters have been obtained from the fit: $\boldsymbol{\sigma_0(\phi \to K^0_L K^0_S) = 1312 \pm 7 \pm 33}$ nb,
$\boldsymbol{M_\phi = 1019.470 \pm 0.013 \pm 0.018}$ MeV, $\boldsymbol{\Gamma_\phi = 4.51 \pm 0.04 \pm 0.02}$ MeV,
$\boldsymbol{\Gamma_{\phi \to ee} \cdot Br(\phi \to K^0_L K^0_S) = (4.181 \pm 0.024 \pm 0.084) \times 10^{-4}}$ MeV.

4 Study of $\phi \to \eta\gamma \to \pi^+\pi^-\pi^0\gamma$ decay

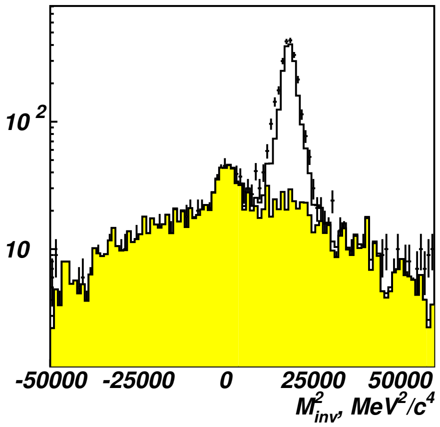

Figure 4: *M^2_{inv} distribution. Points with errors present the data. The hatched histogram is the sum of such distributions for simulation of background processes, solid line histogram is the simulation of $\eta\gamma \to \pi^+\pi^-\pi^0\gamma$ together with background simulation*

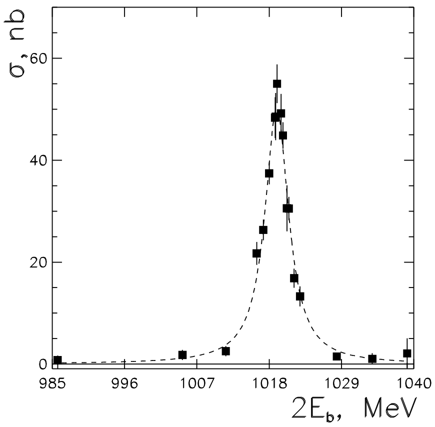

Figure 5: *The cross-section $\sigma(e^+e^- \to \phi \to \eta\gamma)$ with fit function*

The radiative magnetic dipole transition of ϕ into η has been studied with the integrated luminosity of about 1.9 pb^{-1}. Events with two charged particles and one recoil photon with the energy more than 250 MeV were selected. The direction of the recoil photon should be close to the opposite direction of two charged pions. The reconstructed invariant mass of all other photons in this system (fig.4) forms a peak near the π^0 mass or near zero corresponding to the events of the η decay into $\pi^+\pi^-\gamma$. The small fraction of the background comes from ϕ decays into $\pi^+\pi^-\pi^0, \omega\pi^0$, $K^0_L K^0_S$ and was subtracted according to the simulation results. Fig.5 shows the energy behavior of the cross section of the process $e^+e^- \to \phi \to \eta\gamma$. Using the branching ratio for the $\phi \to e^+e^-$ decay from PDG[16], the following value for branching ratio has been determined: $\boldsymbol{Br(\phi \to \eta\gamma) = (1.18 \pm 0.03 \pm 0.06) \times 10^{-4}}$.

5 Process $e^+e^- \to \eta\gamma \to \pi^0\pi^0\pi^0\gamma$

The reaction $e^+e^- \to \eta\gamma$ when η decays into $3\pi^0$ has been studied in the energy range from 0.6 to 1.4 GeV with the integrated luminosity about 21 pb^{-1}. The preliminary results of measurement of the cross section of the process are shown in fig.6. The curve in this figure shows the fit of the energy dependence of the cross section which takes into account the interference of ρ, ω and ϕ mesons in the intermediate state. The following branching ratios were obtained from the fit:

$\boldsymbol{Br(\phi \to \eta\gamma) = (1.24 \pm 0.02 \pm 0.08) \cdot 10^{-2}}$,
$\boldsymbol{Br(\omega \to \eta\gamma) = (5.6^{+1.2}_{-1.1}) \cdot 10^{-4}}$,
$\boldsymbol{Br(\rho \to \eta\gamma) = (2.1^{+0.6}_{-0.5}) \cdot 10^{-4}}$

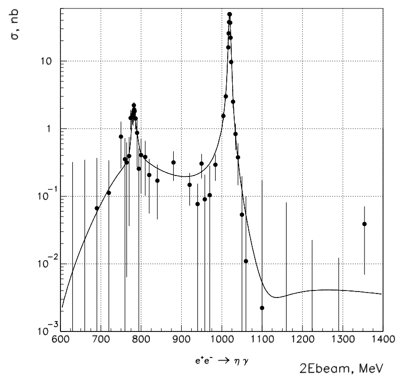

Figure 6: *Cross section of the process* $e^+e^- \to \eta\gamma \to 7\gamma$

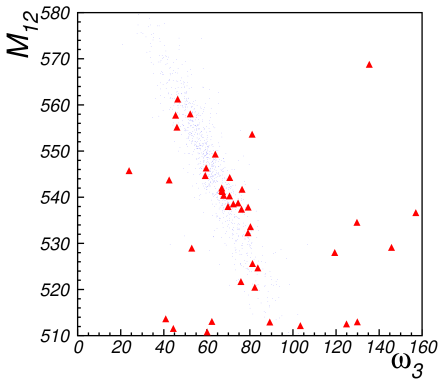

Figure 7: *Invariant mass of two hard photons* M_{12} *vs softest photon energy* ω_3*. Points present the simulation of* $\phi \to \eta'\gamma, \eta' \to \pi^+\pi^-\eta, \eta \to \gamma\gamma$*, triangles — data after all the selections.*

6 Observation of $\phi \to \eta'\gamma$ decay

A search of this rare radiative decay was performed with the integrated luminosity of about 14
$mboxpb^{-1}$ at 14 energy points around the ϕ meson when η' decays into $\pi^+\pi^-\eta$. The analysis of events has been performed using three different decay modes of η: a. $\eta \to \gamma\gamma$, b. $\eta \to \pi^+\pi^-\gamma$ and c. $\eta \to \pi^+\pi^-\pi^0$.

For the first case (a), there are two charged pions and three photons in the final state. The monochromatic recoil photon has a fixed energy of 60 MeV. The invariant mass of two other (more hard) photons should equal M_η. Fig.7 shows the distribution of the invariant mass of two hard photons M_{12}

versus the softest photon energy ω_3. The main source of the background comes from the decay $\phi \to \eta\gamma$ when η decay into $\pi^+\pi^-\pi^0$. In this case the final state has the same particles but their kinematics is drastically different. The hardest photon is monochromatic with the energy 362 MeV and the invariant mass of two others is M_{π^0}. The decay $\phi \to \eta\gamma$ is two orders of magnitude more probable. The branching ratio of $Br(\phi \to \eta'\gamma)$ was calculated relative to $Br(\phi \to \eta\gamma)$. This ratio is not sensitive to systematic uncertainties from luminosity, detector inefficiency, resolution and so on. Using the values of the all needed branching ratios from PDG[16] the following result has been obtained: $\boldsymbol{Br(\phi \to \eta'\gamma) = (0.82^{+0.21}_{-0.19} \pm 0.11) \times 10^{-4}}$.

For the second(b) and third(d) decay modes of η there are four charged particles and two or three photons in the final state. The softest photon is monochromatic with the energy of 60 MeV. One of the combinations of two particles with opposite charges has to form a missing mass to M_{π^0} or zero. The kinematic constrained fit with additional angular cuts was applied to select events with the best χ^2. The main source of the background comes from decays: $\phi \to K^0_S K^0_L$ when $K^0_S \to \pi^+\pi^-$ and $K_L \to \pi^+\pi^-\pi^0$. The number of these background events was subtracted according to the simulation results. The following result has been obtained : $\boldsymbol{Br(\phi \to \eta'\gamma) = (0.58 \pm 0.18 \pm 0.15) \times 10^{-4}}$.

7 Direct observation of $K^0_S \to \pi e\nu$ decay

While the semileptonic decays of K^0_L have been well measured, the information on the similar decays of K^0_S is extremely scarce. PDG evaluates the corresponding decay rate indirectly using the K^0_L semileptonic decays and assuming the rule: ΔS=ΔQ.

We present results of the direct measurement of the branching ratio for $K^0_S \to \pi e\nu$ decay using the unique opportunity to study events containing a pure $K^0_L K^0_S$ system in the final state produced in the reaction: $e^+e^- \to \phi \to K^0_L K^0_S$. The data with the integrated luminosity of 14.8 pb^{-1} were used for this analysis. Fig.8 shows the distribution of the selected events over the parameter $DPE = p - E_{loss} - E_{CsI}$, where p is the particle momentum measured in drift chamber, E_{CsI} is the energy deposition in CsI calorimeter and E_{loss} is the an ionization energy loss in the material in front of CsI calorimeter. An enhancement in this distribution around zero corresponds to the electrons from the decay $K^0_S \to \pi e\nu$. After background subtraction the corresponding number of the events was found to be: $N = 75 \pm 13$. Using the $K^0_S \to \pi^+\pi^-$ decay for normalization, the following branching ratio was obtained: $\boldsymbol{Br(K^0_S \to \pi e\nu)} =$

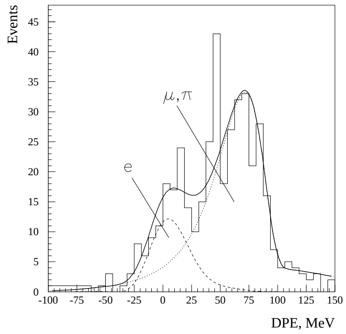

Figure 8: *DPE distribution for charged particles in K_S^0 decays; dashed line — electrons; dotted line — muons and pions*

$\mathbf{(7.19 \pm 1.35) \times 10^{-4}}$. This result is consistent with the PDG value obtained by recalculation from K_L^0 semileptonic rates. More details on the analysis can be found in[13].

8 Study of the conversion decays

Conversion decays, when a virtual photon is converted into a lepton pair, are closely related to corresponding radiative decays. The branching ratios for conversion decays $\phi \to \eta e^+e^-$, $\phi \to \pi^0 e^+e^-$ as well as Dalitz decay $\eta \to e^+e^-\gamma$ were determined using a data sample with the integrated luminosity of 15.5 pb^{-1}.

The decay $\phi \to \eta e^+e^-$ was detected via the mode $\eta \to \gamma\gamma$ and $\eta \to 3\pi^0$, the decay $\phi \to \pi^0 e^+e^-$ – via the $\pi^0 \to \gamma\gamma$ and the decay $\eta \to e^+e^-\gamma$ – via the mode $\phi \to \eta\gamma$. The process $\phi \to \eta\gamma$, $\eta \to \pi^+\pi^-\gamma$ was used to determine the number of ϕ-mesons.

Events were selected with two charged particles in DC and photons in the calorimeter. These events were subject to the kinematic fit with energy-momentum conservation. The conversion decays have a peculiar feature of their kinematics: the angle between e^+ and e^- is as a rule close to zero.

The significant background for these events comes from the γ-quantum conversion in the detector material. The detection efficiencies for these processes were determined by simulation. The decay $\phi \to \pi^0 e^+e^-$ has background from $\phi \to \pi^+\pi^-\pi^0$ via the same final state. This background was suppressed by using the information about energy deposition by electrons and pions in the calorime-

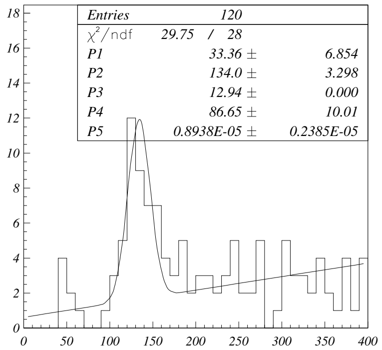

Figure 9: *Distribution over the invariant mass of pair of photons for the process* $\phi \to \pi^0 e^+ e^-$

ter. Fig.9 shows the distribution over the invariant mass of pair of photons for the events of the process $\phi \to \pi^0 e^+ e^-$. As a preliminary result the following branching ratios were obtained:
$\boldsymbol{Br(\phi \to \eta e^+ e^-) = (1.01 \pm 0.14 \pm 0.15) \times 10^{-4}}$ when $\eta \to \gamma\gamma$,
$\boldsymbol{Br(\phi \to \eta e^+ e^-) = (1.20 \pm 0.22 \pm 0.18) \times 10^{-4}}$ when $\eta \to \pi^0\pi^0\pi^0$,
$\boldsymbol{Br(\phi \to \pi^0 e^+ e^-) = (1.23 \pm 0.33 \pm 0.20) \times 10^{-5}}$, $\boldsymbol{Br(\eta \to e^+ e^- \gamma) = (6.85 \pm 0.60 \pm 1.00) \times 10^{-3}}$. The obtained results are in agreement with the theoretical predictions and have better statistical accuracy than previous measurements quoted by PDG.

9 Reactions $e^+e^- \to \pi^+\pi^-\pi^+\pi^-$ and $e^+e^- \to \pi^+\pi^-\pi^0\pi^0$

The reaction of e^+e^- annihilation into four pions (with two possible channels $\pi^+\pi^-\pi^+\pi^-$ and $\pi^+\pi^-\pi^0\pi^0$) was studied in the energy range 1.05–1.38 GeV. Simultaneous analysis of both modes allowed to establish that the final state $\pi^+\pi^-\pi^0\pi^0$ is dominated by a mixture of $\omega\pi^0$ and $a_1(1260)\pi$ mechanisms whereas only the latter contributes to the $\pi^+\pi^-\pi^+\pi^-$ final state[14]. The reaction $e^+e^- \to \pi^+\pi^-\pi^+\pi^-$ was also studied in the energy range 0.6–0.97 GeV[15]. The energy dependence of the cross section in this range agrees with the assumption of the $a_1(1260)\pi$ intermediate state. Fig.10 shows the energy behavior of the cross section of the reaction $e^+e^- \to \pi^+\pi^-\pi^+\pi^-$ in the energy range 0.6 to 2 GeV. Also shown in this figure are the measurements of other groups. For the first time $\pi^+\pi^-\pi^+\pi^-$ events were observed at the ρ meson energy. Under the

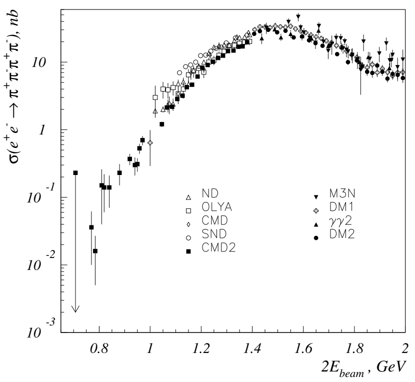

Figure 10: *Cross section of the reaction* $e^+e^- \rightarrow \pi^+\pi^-\pi^+\pi^-$

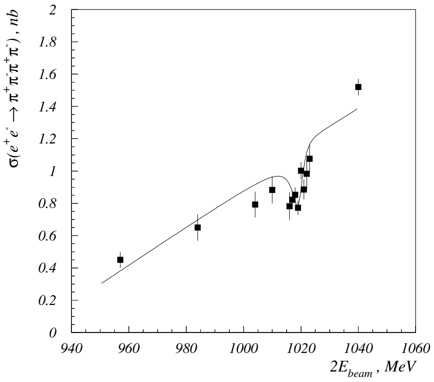

Figure 11: *Cross section of the process* $e^+e^- \rightarrow \pi^+\pi^-\pi^+\pi^-$ *in the* ϕ *meson region*

assumption that all these events come from ρ meson decay, the following value of the decay width was obtained:

$\mathbf{\Gamma(\rho^0 \rightarrow \pi^+\pi^-\pi^+\pi^-) = (2.8 \pm 1.4 \pm 0.5)}$ keV

or the branching ratio:

$\boldsymbol{Br(\rho^0 \rightarrow \pi^+\pi^-\pi^+\pi^-) = (1.8 \pm 0.9 \pm 0.3) \cdot 10^{-5}}$

Fig.11 shows the preliminary results of measurement of the cross section of the process $e^+e^- \rightarrow \pi^+\pi^-\pi^+\pi^-$ near ϕ meson. A signal of the decay $\phi \rightarrow \pi^+\pi^-\pi^+\pi^-$ is well seen in this figure. The following branching ratio was obtained from the fit:

$\boldsymbol{Br(\phi \rightarrow \pi^+\pi^-\pi^+\pi^-) = (5.4 \pm 1.6 \pm 2.0) \cdot 10^{-6}}$

10 Reaction $e^+e^- \rightarrow \pi^+\pi^-\pi^+\pi^-\pi^0$

The energy dependence of the cross section of the process $e^+e^- \rightarrow \pi^+\pi^-\pi^+\pi^-\pi^0$ was measured. The dominance by the contributions from the $\eta\pi^+\pi^-$ and $\omega\pi^+\pi^-$ states was shown. The reaction $e^+e^- \rightarrow \eta\pi^+\pi^-$ was also studied when η decays into $\gamma\gamma$. The results of measurements are shown in fig.12 and 13.

11 Conclusion

New interesting results were obtained with CMD-2 detector on VEPP-2M collider. Among them are the high precision measurement of the cross section

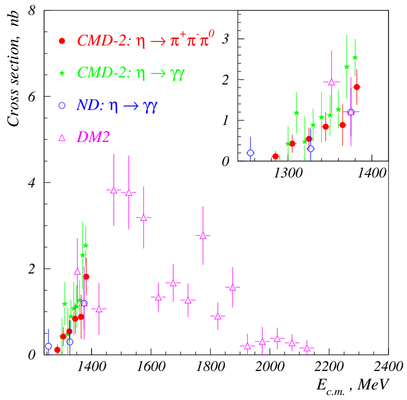

Figure 12: *Cross section of the reaction* $e^+e^- \to \eta\pi^+\pi^-$

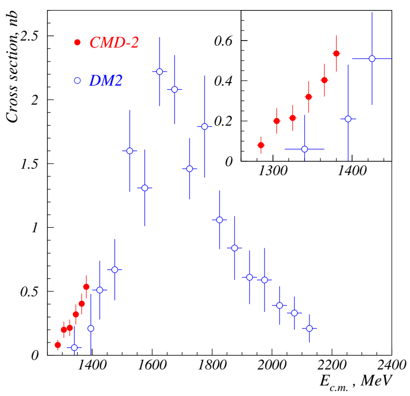

Figure 13: *Cross section of the process* $e^+e^- \to \omega\pi^+\pi^-$

of e^+e^- annihilation into hadrons in the energy range from the threshold of hadron production to 1.4 GeV, investigation of exclusive hadron channels as well as decays of ρ, ω and ϕ mesons. Some of these results are outlined in the tab.2. Analysis is in progress to produce final results with a low systematic uncertainty to meet the original goals of CMD-2.

This work is supported in part by the grants: RFBR-98-02-17851, RFBR-99-02-17053, RFBR-99-02-17119, INTAS 96-0624.

References

[1] S.Eidelman and F.Jegerlehner, Z. Phys. **C67** (1995) 585.

[2] D.H.Broun and W.A.Worstell, Phys.Rev., **D54** (1996) 3237.

[3] G.A.Aksenov et al., Preprint BINP 85-118, Novosibiresk, 1985.

[4] V.V.Anashin *et al.,* Preprint BINP 84-114, Novosibiresk, 1984.

[5] F.V.Ignatov et al., Preprint BINP 99-64, Novosibirsk, 1999.

[6] E.V.Anashkin et al., Nucl. Instr. and Meth., **A323** (1992) 178.

[7] V.M.Aulchenko et al., Nucl. Instr. and Meth., **A336** (1993) 53.

[8] D.N.Grigoriev et al., IEEE Trans. Nuc. Sci., 42, **N4** (1995) 505.

[9] G.A.Aksenov et al., Preprint BINP 85-118, Novosibirsk, 1985.

Table 2: *Results of CMD-2 experiments*

	CMD-2 Data	PDG'98
m_ω, MeV	$782.71 \pm 0.07 \pm 0.04$	781.94 ± 0.12
Γ_ω, MeV	$8.68 \pm 0.23 \pm 0.20$	8.41 ± 0.09
$\Gamma_{\omega \to e^+e^-}$, keV	$0.605 \pm 0.014 \pm 0.010$	0.60 ± 0.02
$Br(\omega \to \pi^+\pi^-)$	$(1.31 \pm 0.23 \pm 0.02) \cdot 10^{-2}$	$(2.21 \pm 0.30) \cdot 10^{-2}$
m_ρ, MeV	$775.28 \pm 0.61 \pm 0.20$	776.0 ± 0.9
Γ_ρ, MeV	$147.70 \pm 1.29 \pm 0.40$	150.5 ± 2.7
$\Gamma_{\rho \to e^+e^-}$, keV	$6.93 \pm 0.11 \pm 0.10$	6.77 ± 0.32
$Br(\rho \to \pi^+\pi^-\pi^+\pi^-)$	$(1.8 \pm 0.9 \pm 0.3) \cdot 10^{-5}$	$< 2 \cdot 10^{-4}$
$Br(\rho \to \eta\gamma)$, $\eta \to 3\pi^0$	$(2.1^{+0.6}_{-0.5}) \cdot 10^{-4}$	$(2.4^{+0.8}_{-0.9}) \cdot 10^{-4}$
$Br(\omega \to \eta\gamma)$, $\eta \to 3\pi^0$	$(5.6^{+1.2}_{-1.1}) \cdot 10^{-4}$	$(6.5 \pm 1.0) \cdot 10^{-4}$
$Br(K^0_S \to \pi e \nu)$	$(7.2 \pm 1.4) \cdot 10^{-4}$	$(6.70 \pm 0.07) \cdot 10^{-4}$
$Br(K^+ \to \pi^+\pi^0)$	$(21.69 \pm 0.48 \pm 1.03) \cdot 10^{-2}$	$(21.16 \pm 0.14) \cdot 10^{-2}$
$Br(K^+ \to \pi^0 e^+ \nu)$	$(4.89 \pm 0.17 \pm 0.17) \cdot 10^{-2}$	$(4.82 \pm 0.06) \cdot 10^{-2}$
$Br(\eta \to e^+e^-\gamma)$	$(6.85 \pm 0.60 \pm 0.90) \cdot 10^{-3}$	$(4.9 \pm 1.1) \cdot 10^{-3}$
$Br(\eta \to \pi^+\pi^-e^+e^-)$	$(3.5 \pm 2.0) \cdot 10^{-4}$	$(13^{+12}_{-8}) \cdot 10^{-4}$
$Br(\eta \to \pi^+\pi^-)$	$< 3.3 \cdot 10^{-4}$	$< 9 \cdot 10^{-4}$
$Br(\eta \to \pi^0\pi^0)$	$< 5 \cdot 10^{-4}$	no data
m_ϕ, MeV	$1019.470 \pm 0.013 \pm 0.018$	1019.413 ± 0.008
Γ_ϕ, MeV	$4.51 \pm 0.04 \pm 0.02$	4.43 ± 0.05
$Br(\phi \to \eta\gamma)$, $\eta \to 3\pi^0$	$(1.24 \pm 0.02 \pm 0.08) \cdot 10^{-2}$	$(1.26 \pm 0.06) \cdot 10^{-2}$
$Br(\phi \to \eta\gamma)$, $\eta \to \pi^+\pi^-\pi^0$	$(1.18 \pm 0.03 \pm 0.06) \cdot 10^{-2}$	$(1.26 \pm 0.06) \cdot 10^{-2}$
$Br(\phi \to e^+e^-)$	$(2.87 \pm 0.09) \cdot 10^{-4}$	$(2.99 \pm 0.08) \cdot 10^{-4}$
$\delta_{\phi-\omega}$	$(162 \pm 17)^\circ$	
$Br(\phi \to \eta'\gamma)$, $\eta' \to \pi^+\pi^-\gamma\gamma$	$(8.2^{+2.1}_{-1.9} \pm 1.1) \cdot 10^{-5}$	$(12^{+7}_{-5}) \cdot 10^{-5}$
$Br(\phi \to \eta'\gamma)$, $\eta' \to \pi^+\pi^-\pi^+\pi^-\pi^0$ or $\eta' \to \pi^+\pi^-\pi^+\pi^-\gamma$	$(5.8 \pm 1.8 \pm 1.5) \cdot 10^{-5}$	$(12^{+7}_{-5}) \cdot 10^{-5}$
$Br(\phi \to \eta e^+e^-)$, $\eta \to \gamma\gamma$	$(1.01 \pm 0.14 \pm 0.15) \cdot 10^{-4}$	$(1.3^{+0.8}_{-0.6}) \cdot 10^{-4}$
$Br(\phi \to \eta e^+e^-)$, $\eta \to \pi^+\pi^-\pi^0$	$(1.00 \pm 0.18) \cdot 10^{-4}$	$(1.3^{+0.8}_{-0.6}) \cdot 10^{-4}$
$Br(\phi \to \eta e^+e^-)$, $\eta \to 3\pi^0$	$(1.20 \pm 0.22 \pm 0.18) \cdot 10^{-4}$	$(1.3^{+0.8}_{-0.6}) \cdot 10^{-4}$
$Br(\phi \to \pi^0e^+e^-)$	$(1.40 \pm 0.33 \pm 0.21) \cdot 10^{-5}$	$< 1.2 \cdot 10^{-4}$
$Br(\phi \to \mu^+\mu^-\gamma)$	$(1.43 \pm 0.45 \pm 0.14) \cdot 10^{-5}$	$(2.3 \pm 1.0) \cdot 10^{-5}$
$Br(\phi \to \rho\gamma)$	$< 1.2 \cdot 10^{-5}$	$< 7 \cdot 10^{-4}$
$Br(\phi \to \rho\gamma\gamma)$	$< 5 \cdot 10^{-4}$	no data
$Br(\phi \to \eta\pi^+\pi^-)$	$< 3 \cdot 10^{-4}$	no data
$Br(\phi \to \pi^+\pi^-\pi^+\pi^-)$	$(5.4 \pm 1.6 \pm 2.0) \cdot 10^{-6}$	$< 8.7 \cdot 10^{-4}$

[10] R.R.Akhmetshin et al., Preprint BINP 99-10, Novosibirsk, 1999.

[11] R.R.Akhmetshin et al., Phys.Lett., **B364** (1995) 199.

[12] R.R.Akhmetshin *et al.*, Phys.Lett., **B466** (1999) 385.

[13] R.R.Akhmetshin *et al.*, Phys.Lett., **B456** (1999) 90.

[14] R.R.Akhmetshin *et al.* hep-ex/9904024 (1999).

[15] R.R.Akhmetshin *et al.* hep-ex/9912020 (1999).

[16] Review of Particle Physics, The European Physical Journal, **C3** (1998).